WIRELESS COMMUNICATIONS AND MOBILE COMPUTING
Wirel. Commun. Mob. Comput. 2008; **8**:995–1009
Published online 10 July 2008 in Wiley InterScience
(www.interscience.wiley.com) DOI: 10.1002/wcm.661

Coverage and connectivity in three-dimensional underwater sensor networks

S. M. Nazrul Alam[1]*,† and Zygmunt J. Haas[2]

[1]*Department of Computer Science, Cornell University, Ithaca, NY, U.S.A.*
[2]*School of Electrical and Computer Engineering, Cornell University, Ithaca, NY, U.S.A.*

Summary

Unlike a terrestrial network, an underwater sensor network can have significant height which makes it a three-dimensional network. There are many important sensor network design problems where the physical dimensionality of the network plays a significant role. One such problem is determining how to deploy minimum number of sensor nodes so that all points inside the network is within the sensing range of at least one sensor and all sensor nodes can communicate with each other, possibly over a multi-hop path. The solution to this problem depends on the ratio of the communication range and the sensing range of each sensor. Under sphere-based communication and sensing model, placing a node at the center of each virtual cell created by truncated octahedron-based tessellation solves this problem when this ratio is greater than 1.7889. However, for smaller values of this ratio, the solution depends on how much communication redundancy the network needs. We provide solutions for both limited and full communication redundancy requirements. Copyright © 2008 John Wiley & Sons, Ltd.

KEY WORDS: three-dimensional; coverage; connectivity; polyhedron; node placement; sphere-based sensing and communication

1. Introduction

In a terrestrial sensor network, the height of the network is usually negligible as compared to its length and width, and as a result a terrestrial network is generally modeled as a two-dimensional (2D) network where it is assumed that all nodes reside on a plane. On the other hand, nodes of an underwater sensor network can be deployed at different depths of the ocean [1]. Such an underwater sensor network can have significant height and it must be modeled as a three-dimensional (3D) network where nodes are distributed over a 3D space. There are many important problems in sensor network design where the physical dimensionality of the network plays a very significant role and the optimal solution of such a problem in a 3D network is quite different from the optimal solution in a 2D network. One such problem is to figure out the minimum number of nodes needed to maintain full coverage (i.e., monitor every points of the network area) and connectivity (i.e., nodes can communicate with each other). Solution to this problem essentially provides a lower bound on the number of nodes needed in a sensor network to achieve full coverage and connectivity. An extensive research has been done on this problem in the context of 2D terrestrial networks.

*Correspondence to: S. M. Nazrul Alam, Department of Computer Science, Cornell University, Ithaca, NY, U.S.A.
†E-mail: smna@cs.cornell.edu

However, since a 3D network is still a novelty, this fundamental problem has largely been unexplored in the context of a 3D network.

Ensuring coverage and connectivity in a 3D network with minimum number of nodes depends on various aspects of the network. In this paper, we focus on the case where communication and sensing ranges of a sensor node are deterministic, omni-directional, and spherical. We also assume that each node has a positioning component to determine its geographical coordinates, and nodes can be placed at any desired position in the 3D space. Many of these assumptions may not be valid in a practical setting, but the solution to the problem based upon these simple assumptions provides us with a theoretical lower bound on the number of nodes required and thus can be very useful to a sensor network designer. Our node placement algorithms can also be used with minor adjustments in a practical underwater deployment.

Under the above assumptions, the solution of our problem depends on the ratio of the communication range and the sensing range. At first, we ignore the limitation on the communication range and find that placing a node at the center of each virtual cell created by truncated octahedron-based tessellation of 3D space solves this problem if the ratio of communication range and sensing range is at least 1.7889 (see Section 5). In this case, full coverage automatically ensures connectivity with all geographically neighboring nodes. However, if the ratio falls below 1.7889, the solution depends on the desired communication redundancy. If we require that all geographically neighboring nodes must be within the communication range of a node, then we have to deploy more nodes than the number of nodes necessary for full coverage. A solution to achieve this objective is provided in Section 6. On the other hand, if we sacrifice full connectivity and instead require at least one path between any two nodes, then the solution is as shown in Section 7. Finally, all the above scenarios have some assumptions that may not be valid in a real underwater sensor network. In Section 8, we discuss how to adjust our theoretical solutions when these assumptions are violated. We conclude the paper in Section 9.

2. Problem Statement

The main assumptions and the goals of our work are defined as follows:

Assumptions:

- Sphere-based sensing: we assume a sphere-based sensing model such that each active sensor has a sensing range of r_s; an active sensor can reliably detect any object that is located within a distance of r_s from the sensor.
- Sphere-based communication: we assume a spherical communication model where each active sensor has a communication range of r_c; if the distance between two active sensors is less than or equal to r_c, then they can communicate reliably with each other.
- Homogeneous sensing and communication range: we assume that all sensors have same sensing range and the communication range of all sensors is also identical.
- No boundary effect: we assume that the network is very large and there is no boundary effect, so that the number of nodes required for a placement strategy is inversely proportional to the volume of a Voronoi cell of the nodes.
- Adjustable node position: we assume that a node can be deployed in any position (or, move to that position) as required by the positioning algorithm. One major criticism of this assumption is that GPS does not work underwater and we do not have any robust positioning mechanism for underwater network yet. However, this assumption ensures that the solution to this problem provides a lower bound on the number of nodes needed to achieve full coverage and connectivity. Knowing the lower bound of the number of nodes is always useful for a designer of an underwater sensor network. It is also possible to adjust the node placement to accommodate small positioning errors.

Goals:

- To find the node placement strategy that achieves full coverage and full connectivity with all first-tier geographically neighboring nodes[‡] with minimum number of sensor nodes in a 3D network for all values of r_c/r_s.
- To find the node placement strategy that achieves full coverage and 1-connectivity[§] with minimum

[‡]Consider virtual Voronoi cells created such that each node is placed at the center of a Voronoi cell. Then we say two nodes are first-tier geographically neighboring nodes, if their corresponding virtual Voronoi cells share a common surface, line, or a point.

[§]A network has k-connectivity if every node can communicate with every other nodes of the network along at least k different node disjoint paths.

DOI: 10.1002/wcm

number of sensor nodes in a 3D network for all values of r_c/r_s.

3. Related Work

The related works of this paper can be classified into two parts: in the context of 2D networks and in the context of 3D networks.

3.1. Related Works in 2D Networks

The problem of providing sensing coverage has received significant attention in the context of 2D sensor networks [2–5]. Maximizing the sensing coverage is a fundamental requirement for many critical applications of sensor networks, for example, detection [6], monitoring, and tracking and classification [7]. Several algorithms have been proposed to achieve full sensing coverage in a 2D network when a sensor network is deployed using random network topology [3,5,8,9]. These results are mostly applicable for 3D networks as well. On the other hand, the problem that we want to solve has been investigated for 2D networks in References [2,5,10]. Under the similar assumptions that has been stated in Section 2,¶ if $r_c/r_s \geq \sqrt{3}$, then placing nodes at the centers of the cells of a regular hexagonal tessellation of a 2D-plane such that each hexagon has radius equal to r_s (or, equivalently, at the vertices of a triangular lattice) provides both full coverage and connectivity with minimum number of sensors [2,5,10]. However, if $r_c/r_s < \sqrt{3}$, then full coverage does not automatically imply connectivity and ensuring connectivity by adjusting the radius of the hexagons requires more nodes than the minimum number of nodes required for full coverage. It has been shown that strip-based deployment (see Figure 1(a)) achieves full coverage and 1-connectivity with minimum number of nodes in 2D when $r_c/r_s < \sqrt{3}$ [2]. The distance between any two neighboring nodes on a strip is set to $\alpha = \min\{r_c, \sqrt{3}r_s\}$. The value of α comes from the fact that in optimal hexagonal-based node placement, the distance between two geographically neighboring nodes is $\sqrt{3}r_s$. Figure 1(b) shows how to determine the value of β, distance between two strips. Clearly,

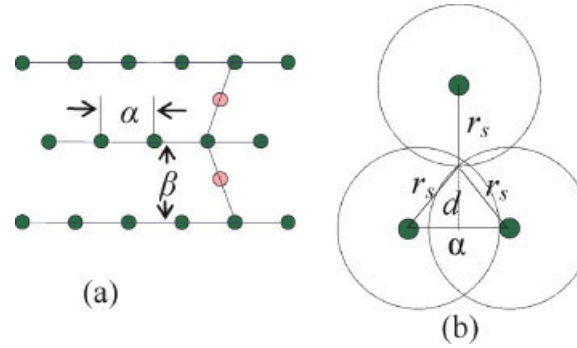

Fig. 1. (a) Strip-based deployment in 2D and (b) calculation of β.

$$\beta = r_s + d = r_s + \sqrt{r_s^2 - \frac{\alpha^2}{4}}$$

In this deployment pattern, connectivity is ensured only among the neighboring nodes in a strip. If $r_c/r_s < \sqrt{3}$, then nodes of two horizontal strips cannot communicate. So a vertical strip is deployed to achieve 1-connectivity in the whole network. It can easily be extended to 2-connectivity by deploying two vertical strips: one in the left boundary of the network and the other in the right boundary of the network. However, 3-connectivity cannot be achieved because in general a node in a horizontal strip can only communicate with two nodes.

The difference between this strip-based approach and the optimal hexagon-based tessellation approach is that the distance along one axis is adjusted to maintain connectivity when $r_c/r_s < \sqrt{3}$. When $r_c/r_s \geq \sqrt{3}$, strip-based node placement degenerates into optimal hexagonal tessellation-based approach and no auxiliary node is needed. We extend this approach for 3D network in Section 7.

3.2. Related Works in 3D Networks

There exist only few references on 3D networks in the literature; the works presented in References [11] and [12] studied 3D cellular networks. In Reference [11], each cell is represented as rhombic dodecahedron and in Reference [12] each cell is represented as hexagonal prism. However, in this paper, we show that if truncated octahedron is used to model the shape of a cell, then the required number of nodes to monitor a 3D space is 43.25 per cent fewer than the case where the cell is represented as hexagonal prism or rhombic dodecahedron, when $r_c/r_s \geq 4/\sqrt{5}$. There is no

¶Note that communication and sensing models are disk based in 2D whereas they are sphere based in 3D.

DOI: 10.1002/wcm

published work that deals with the problem when $r_c/r_s < 4/\sqrt{5}$.

It has been shown that body-centered cubic (BCC) lattice has the smallest mean squared error of any lattice quantizer in three dimensions [13] which implies that placing nodes in a BCC lattice structure is the optimal way to achieve full coverage with minimum number of nodes. Using a different approach, similar result has been obtained in Reference [14], which shows that full coverage and full connectivity with all geographically neighboring nodes using minimum number of nodes can be achieved by placing a node at the center of each cell of a truncated octahedron tessellation of a 3D space (or, equivalently, at the vertices of a BCC lattice) where the radius of a cell is equal to the sensing range. However, connectivity is not an issue in Reference [13], as it is not written in the networking context. Consequently, [13] is not relevant when we have to deal with the scenario where $r_c/r_s < 4/\sqrt{5}$. On the other hand, we can easily modify the approach of Reference [14] to analyze the scenario where $r_c/r_s < 4/\sqrt{5}$. So in this paper, at first we briefly present the approach of Reference [14] and then proceed to solve the problem for all values of r_c/r_s.

4. Preliminaries

In this section, we define some relevant terms and provide some background information necessary to explain our solution approach.

4.1. Space-Filling Polyhedron

A polyhedron is a 3D shape consisting of finite number of polygonal faces. The faces meet in straight line segments called edges, and the edges meet at points called vertices of the polyhedron. A polyhedron surrounds a bounded volume in three-dimensions. Example of polyhedrons includes cube, prisms, and pyramids. Polygon is a 2D analog of polyhedrons. The general term for any dimension is polytope.

A space-filling polyhedron is a polyhedron that can be used to fill a volume without any overlap or gap (a.k.a. tessellation or tiling). Since the sensing region of a node is spherical and spheres do not tessellate in 3D, in order to minimize the number of nodes, we want to find a space-filling polyhedron that best approximates the sphere. In other words, we want to find a space-filling polyhedron such that if each cell is modeled by that polyhedron, then the number of cells required to cover a volume is minimized, where the distance from the center of a cell to its farthest corner (i.e. radius of a cell) is not greater than the sensing range r_s.

At first, we provide a short overview on space-filling polyhedron. It is not easy to show that a polyhedron has space-filling property. For example, although Aristotle claimed that the tetrahedron fills space [15], his claim was incorrect [16], and the mistake remained unnoticed until the 16th century [17].

Some of the important results on space-filling polyhedron are as follows: there are exactly five regular polyhedrons (a.k.a. platonic solids or regular solids) [18]: cube, dodecahedron, icosahedron, octahedron, and tetrahedron, as was proved by Euclid in the last proposition of the *Elements*. Among them, only cube has the space-filling property [19]. There are only five convex polyhedrons with regular faces having space-filling property: triangular prism, hexagonal prism, cube, truncated octahedron [18,20], and gyrobifastigium [21]. The rhombic dodecahedron, elongated dodecahedron, and squashed dodecahedron are also space fillers. A combination of tetrahedrons and octahedrons fills space. In addition, octahedrons, truncated octahedrons, and cubes, combined in the ratio 1:1:3, can also fill space.

However, we impose the restriction that the shape of the Voronoi cells should be identical, that is, only one type of polyhedron is used to fill the space. While a homogeneous tiling is not necessarily the best pattern in deriving an optimal pattern, it is considered here because of the following two reasons:

- algorithms, especially distributed algorithms, to find the location of nodes are far simpler when one type of polyhedron is used, and
- since the radius of the polyhedron is fixed, it is unlikely that any significant improvement can be achieved by using two or more type of polyhedrons to fill the space.

4.2. Kelvin's Conjecture

Now we describe the century old Kelvin's conjecture that we use to justify why truncated octahedron is the building block for the optimal solution in Section 5.

In 1887, Lord Kelvin asked the following question [22]: '*What is the optimal way to fill a three dimensional space with cells of equal volume, so that the surface area (interface area) is minimized?*' This is essentially the problem of finding a space-filling structure having the highest *isoperimetric quotient*.

DOI: 10.1002/wcm

If the volume and surface area of a structure are V and S, respectively, then in three-dimensions its isoperimetric quotient can be defined as $36\pi V^2/S^3$. Sphere has the highest isoperimetric quotient and it is 1. Kelvin's answer to his question was 14-sided truncated octahedron having a very slight curvature of the hexagonal faces and its isoperimetric quotient is 0.757. But Kelvin could not prove that the structure is optimal. The uncurved truncated octahedron has isoperimetric quotient of 0.753367. For more than a century, Kelvin's solution was generally accepted as correct [23] and has been widely known as *Kelvin's conjecture*. But in 1994, two physicists Denis Weaire and Robert Phelan came up with another space-filling structure. It consists of six 14-sided polyhedrons and two 12-sided polyhedrons with irregular faces of equal volume that has 0.3 per cent less surface area than truncated octahedron [24,25]. The isoperimetric quotient of this structure is 0.764. But any proof that the structure of Weiare and Phelan is optimal or that Kelvin's solution is optimal for the case when the cells are identical is yet to be found.

4.3. Voronoi Tessellation

In three-dimension, for any (topologically) discrete set S of points in Euclidean space, the set of all points closer to a point c of S than to any other point of S is the interior of a convex polyhedron called the *Voronoi cell* of c. The set of such polyhedrons tessellate the whole space, and is called the *Voronoi tessellation* corresponding to the set S. Voronoi tessellation of any solution to our problem of the optimal location of the nodes, gives the optimal shape of each cell.

5. Full Coverage and Connectivity When $r_c/r_s \geq 4/\sqrt{5}$

In this section, we analyze our problem from the point of view of the shape of Voronoi cells corresponding to the placement of nodes in the network. If each Voronoi cell is identical and the boundary effect is negligible, then total number of nodes required for 3D coverage is simply the ratio of the volume of the 3D space to be covered to the volume of one Voronoi cell. So minimizing the number of nodes can be achieved if the Voronoi cells have the highest volume for the given sensing radius r_s. Clearly, the radius of the circumsphere of a Voronoi cell must be less than or equal to the sensing range r_s. Since achieving the highest volume is the goal, the radius of circumsphere must always be equal to the sensing range r_s. Furthermore since r_s is fixed, the volumes of the circumspheres of all Voronoi cells are the same and equal to $4\pi r_s^3/3$. Finally, the shape of any Voronoi cell in 3D is always a polyhedron. The restriction of identical Voronoi cell implies that the shape of all cells will be the same polyhedron. Clearly, the polyhedron must have the space-filling property. So our problem reduces to the problem of finding the space-filling polyhedron which has the highest ratio of its volume to the volume of its circumsphere. We call this ratio the *volumetric quotient* of the space-filling polyhedron. More formal definition is as follows:

Definition. *For any polyhedron, if the maximum distance from its center to any vertex is r_s and the volume of that polyhedron is V, then the volumetric quotient of that polyhedron is* $3V/4\pi r_s^3$.

Since the volume of the circumsphere is the upper bound on the volume of any polyhedron, the value of volumetric quotient is always between 0 and 1. Clearly, for a given sensing range r_s, the number of nodes required to cover a 3D space is inversely proportional to the volumetric quotient of the space-filling polyhedron used as a Voronoi cell. So our problem reduces to the problem of finding the space-filling polyhedron that has the highest volumetric quotient.

One possible approach is to check all possible space-filling polyhedrons and determine which space-filling polyhedron has the highest volumetric quotient. However, a rigorous proof that considers all possible space-filling polyhedrons is intractable, as is evident from the fact that Kelvin's problem for the case of a single cell shape is still open for more than a century. So, instead, at first we provide some intuition why truncated octahedron is the most likely solution by drawing similarity between our problem and Kelvin's conjecture. Then we choose three other different space-filling polyhedrons that have been used by other researchers in similar problems and which are reasonable contenders of truncated octahedron. We provide detail comparison among these four space-filling polyhedrons and we show that truncated octahedron has much higher volumetric quotient than others.

5.1. Similarity With Kelvin's Conjecture

Kelvin's problem is essentially finding a space-filling polyhedron that has the highest isoperimetric quotient

DOI: 10.1002/wcm

and our problem is essentially finding a space-filling polyhedron that has the highest volumetric quotient. Among all 3D shapes, sphere has the highest isoperimetric quotient and volumetric quotient and in both cases that value is 1. We conjecture that for any two space-filling polyhedrons P_1 and P_2, if P_1 has higher isoperimetric quotient than P_2, then P_1 also have higher volumetric quotient than P_2. Clearly, it is true if we compare any 3D shape with sphere. If this conjecture is true, then the solution to Kelvin's problem is essentially the solution to our problem. Since until now, truncated octahedron is the best solution for Kelvin's problem for the case of identical cells, we conjecture that truncated octahedron is the most likely solution to our problem as well. Note that we will consider the uncurved version of the truncated octahedron because it is mathematically more tractable than the curved version and the difference between the curved version and the uncurved version is negligible. Because the argument given above is not rigorous enough, to increase the confidence in our solution, we choose other likely contenders to the truncated octahedron, and we provide comparison of the truncated octahedron with those other space-filling polyhedrons.

5.2. Choice of Other Polyhedrons

Kepler's conjecture for sphere packing problem has been proven recently after five centuries of efforts, with the FCC lattice being the solution to that problem[‖] [26]. The Voronoi tessellation of the FCC lattice is rhombic dodecahedron. One can try to solve our problem using Kepler's problem in the following way. Find the maximal packing of spheres and then take the Voronoi tessellation corresponding to the centers of the spheres. Take the radius of spheres such that the maximum distance from a center to any vertex of the corresponding Voronoi cell is the sensing range r_s. So we choose rhombic dodecahedron as one of the contender to the truncated octahedron.

The solution to our problem in 2D is the hexagon. The polyhedron that has hexagon as its cross-section in all the three axes (i.e., x-, y-, and z-axes) does not have space-filling property. Two polyhedrons that have space-filling property and each has at least one hexagonal cross-section are rhombic dodecahedron and hexagonal prism. So we include hexagonal prism in our comparison as well. Another reason is that two previous works use rhombic dodecahedron [11] and hexagonal prism [12] as the shape of the cell in the context of 3D cellular network. Finally, most simplistic choice is the cube and it is the only regular polyhedron that tessellates a 3D space. For notational convenience, we call cube, hexagonal prism, rhombic dodecahedron, and truncated octahedron-based tessellation and node placement as CB, HP, RD, and TO model, respectively. In the next subsection, we compare all four models and find that the truncated octahedron has higher volumetric quotient than other choices, hence TO model requires the fewest number of nodes. Note that Reference [13] provides a proof that implies that TO model actually requires the fewest number of nodes. However, still we provide this discussion because it allows us to extend this work to solve the problem for all values of r_c/r_s in Section 6, whereas Reference [13] does not consider connectivity and so their proof approach cannot be used to solve that problem.

5.3. Volumetric Quotient and Number of Nodes Required by Different Models

Here, we calculate the volumetric quotients of our chosen polyhedrons and also provide a comparison of the number of nodes required when each of the polyhedrons is used as Voronoi cells.

5.3.1. Cube (CB)

If the length of each side of a cube is a, then the radius of its circumsphere is $\sqrt{3}a/2$. So the volumetric quotient of a cube is

$$a^3 \Big/ \frac{4}{3}\pi\left(\frac{\sqrt{3}}{2}a\right)^3 = \frac{2}{\sqrt{3}\pi} = 0.36755$$

5.3.2. Hexagonal prism (HP)

The volumetric quotient of a hexagonal prism depends on its height. So at first we need to find out the optimal height of a hexagonal prism which has the largest volumetric quotient among all the hexagonal prisms. Suppose that the length of each side of the hexagon is a and the height of the hexagonal prism is h (see Figure 2). Then the radius of circumsphere of the

[‖]Finding the densest packing of spheres is known as the Kepler problem.

DOI: 10.1002/wcm

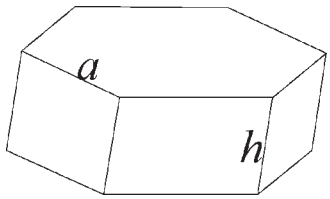

Fig. 2. A hexagonal prism.

hexagonal prism is $\sqrt{a^2+h^2/4}$, the volume of the hexagonal prism is $3\sqrt{3}a^2h/2$, and the volumetric quotient is $(3\sqrt{3}/2)a^2h/\frac{4}{3}\pi\left(\sqrt{a^2+(h^2/4)}\right)^3$.

If we set the first derivative of the volumetric quotient to zero, then we obtain that

$$\frac{(3\sqrt{3}/2)a^2}{\frac{4}{3}\pi\left(\sqrt{a^2+h^2/4}\right)^3}-\frac{3}{2}\frac{(3\sqrt{3}/2)a^2h\cdot(2h/4)}{\frac{4}{3}\pi\left(\sqrt{a^2+h^2/4}\right)^5}=0$$

$$\Rightarrow a^2+\frac{h^2}{4}=\frac{3h^2}{4}$$

So, the optimum value of h is $a\sqrt{2}$ and the optimum volumetric quotient of hexagonal prism is

$$\frac{3\sqrt{3}}{2}a^2a\sqrt{2}\Big/\frac{4}{3}\pi\left(\sqrt{a^2+\frac{a^2}{2}}\right)^3=\frac{6}{4\pi}=0.477$$

5.3.3. Rhombic dodecahedron (RD)

A rhombic dodecahedron can be constructed from two identical cubes in the following way, shown in Figure 3.

Take one cube and cut it into six equal pyramids such that the base of each pyramid consists of one face of the cube. Take another similar cube and place each pyramid on the cube, such that the base of the pyramid is on one side of the cube. This creates a rhombic dodecahedron. If each side of the two original cubes is a (i.e., length of each edge of the rhombic dodecahedron is $\sqrt{3}a/2$), then total volume of the rhombic dodecahedron is $2a^3$. The center of the rhombic dodecahedron is the center of the second (intact) cube. Eight vertices of the intact cube form eight vertices of the rhombic dodecahedron and their distance from the center is the radius of the circumsphere of the cube, equal to $\sqrt{3}a/2$. The other six vertices of the rhombic dodecahedron are formed by the six pieces of the first cube. Distance from the center of second cube to its surface is $a/2$ and the height of each of the six pyramids is $a/2$. So the distance from the center of a rhombic dodecahedron to each of these six vertices is a, and this is also the radius of the circumsphere of the rhombic dodecahedron. So the volumetric quotient of rhombic dodecahedron is $2a^3/\frac{4}{3}\pi a^3=6/4\pi=0.477$, which is exactly the same as that of the hexagonal prism.

5.3.4. Truncated octahedron (TO)

Truncated octahedron has 14 faces, of which 8 are hexagonal and 6 are square faces, and the length of the edges of hexagons and squares are the same. Suppose that the length of each edge is a. The distance between two opposite hexagonal faces is $\sqrt{6}a$ and the distance between two opposite square faces is $2\sqrt{2}a$. The radius of the circumsphere of the truncated octahedron is $\sqrt{10}a/2$. The volume of the truncated octahedron is $8\sqrt{2}a^3$ and the volumetric quotient is

$$8\sqrt{2}a^3\Big/\frac{4}{3}\pi\left(\frac{1}{2}\sqrt{10}a\right)^3=24\Big/5\sqrt{5}\pi=0.68329$$

Truncated octahedron tessellation of a 3D space is shown in Figure 4.

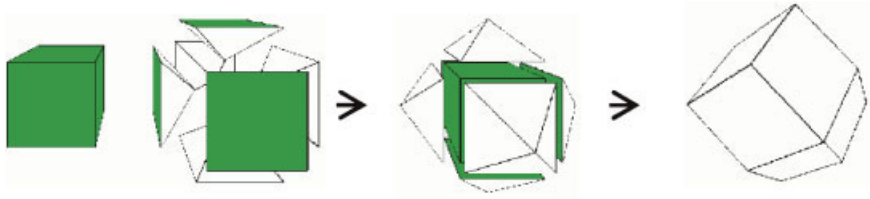

Fig. 3. Construction of a rhombic dodecahedron from two identical cubes.

DOI: 10.1002/wcm

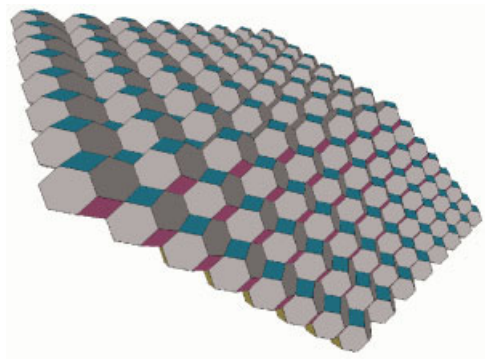

Fig. 4. Truncated octahedron tessellation of a 3D space.

5.3.5. Comparison

Among all the polyhedrons considered, the truncated octahedron gives the best volumetric quotient. Since volumetric quotient is inversely proportional to the number of nodes required to cover a 3D space, we can also compare the number of nodes required by each models. Table I shows these numbers.

5.3.6. Explanation of why truncated octahedron is better

Cross-sections of the rhombic dodecahedron and the hexagonal prism are hexagons, but the vertices of this hexagon are not on the great circle of the circumsphere. As a result, the radius of the hexagon is smaller than the sensing range. In the case of truncated octahedron, the 2D tiling is by octagons that lies on the great circle. But 2D tiling by regular octagon has square gaps. These square gaps are filled in 3D by cells from one level above and one level below. As a result, for a given sensing range and sufficiently high communication range (i.e., $r_c/r_s \geq 4/\sqrt{5}$), TO model requires fewest node to cover a given 3D space.

5.4. Placement Strategies

In this subsection, we provide strategies (algorithms) to pinpoint the location where the nodes should be placed such that the Voronoi cells are our chosen space-filling polyhedrons. We take an arbitrary point and place a node there. Then we find the locations of other nodes relative to this center node. So the input to our algorithm is sensing range r_s (so the radius of a cell is $R = r_s$) and the co-ordinates of a point, say (x, y, z), which act as a seed for the growing lattice. This can be done in a distributed manner by first selecting a leader using any standard leader selection algorithm [27] and then the location of the leader can be used as the seed. Here, we assume that nodes already have information about the orientation of x, y, and z-axes from their localization component.

Table I. Volumetric quotient and (relative) number of nodes needed by different models.

Model	Volumetric quotient	Number of nodes needed (per cent)
CB	0.36755	185.9
HP	0.477	143.25
RD	0.477	143.25
TO	0.68329	100

To save space, here we briefly present the results. Details derivation can be found in Reference [14]. CB, HP, RD, and TO placement can be achieved in the following way: take any arbitrary point (x, y, z) as the center of the network and deploy one node in co-ordinates

$$\text{For CB: } \left(x + u\frac{2R}{\sqrt{3}}, y + v\frac{2R}{\sqrt{3}}, z + w\frac{2R}{\sqrt{3}}\right) \quad (1)$$

$$\text{For HP: } \left(x + uR\sqrt{\frac{3}{2}}, y + (u + 2v)\frac{R}{\sqrt{2}}, z + \frac{2Rw}{\sqrt{3}}\right) \quad (2)$$

$$\text{For RD: } \left(x + (2u + w)\frac{R}{\sqrt{2}}, y + (2v + w)\frac{R}{\sqrt{2}}, z + wR\right) \quad (3)$$

$$\text{For TO: } \left(x + (2u + w)\frac{2R}{\sqrt{5}}, y + (2v + w)\frac{2R}{\sqrt{5}}, z + w\frac{2R}{\sqrt{5}}\right) \quad (4)$$

where $u \in Z$, $v \in Z$, $w \in Z$; Z is the set of integers (both negative and positive).

Clearly, this approach deploys nodes in the entire 3D Euclidean space. In practice, 3D networks will be finite and node placement can be made for a finite network by considering only those co-ordinates that fall within the space that we want to cover. Same discussion applies to other contexts in this paper where we refer to Z.

Real distance between any two nodes with values of u, v, w as u_1, v_1, w_1 and u_2, v_2, w_2 is as follows:

DOI: 10.1002/wcm

$$\text{For CB: } d_{12}^{\text{CB}} = \frac{2}{\sqrt{3}} R \sqrt{(u_2 - u_1)^2 + (v_2 - v_1)^2 + (w_2 - w_1)^2}$$

$$\text{For HP: } d_{12}^{\text{HP}} = R\sqrt{2}\sqrt{(u_2 - u_1)^2 + (u_2 - u_1)(v_2 - v_1) + (v_2 - v_1)^2 + \tfrac{2}{3}(w_2 - w_1)^2}$$

$$\text{For RD: } d_{12}^{\text{RD}} = R\sqrt{2}\sqrt{(u_2 - u_1)^2 + (v_2 - v_1)^2 + (w_2 - w_1)^2 + (u_2 - u_1)(w_2 - w_1) + (v_2 - v_1)(w_2 - w_1)}$$

$$\text{For TO: } d_{12}^{\text{TO}} = \frac{4}{\sqrt{5}} R \sqrt{(u_2 - u_1)^2 + (v_2 - v_1)^2 + (u_2 - u_1)(w_2 - w_1) + (v_2 - v_1)(w_2 - w_1) + \tfrac{3}{4}(w_2 - w_1)^2}$$

Figure 5 shows node placement under CB, HP, RD, TO models using Equations (1), (2), (3), and (4), respectively. This illustration is done in *C* using OpenGL.

5.5. Communication Range *Versus* Sensing Range

The required minimum communication range r_c to maintain connectivity among geographically neighboring nodes is different for different models. In each case, if we consider a new 3D co-ordinate system where integer coordinates (u, v, w) represents the location of each node, then the distance between two geographically neighboring nodes are essentially unit distance along u, v, and w-axes. In CB model, the distance between any two neighboring node along u, v, and w-axes is $2r_s/\sqrt{3}$. Thus, we must have $r_c/r_s \geq 2\sqrt{3} = 1.1547$. In HP model, we must have $r_c/r_s \geq \sqrt{2} = 1.4142$ to maintain connectivity with the neighbors along the axes u and v, and $r_c/r_s \geq 2/\sqrt{3} = 1.1547$ along the w-axis. In RD model, we need $r_c/r_s \geq \sqrt{2} = 1.4142$ along all three axes. Finally, in TO model, we need $r_c/r_s \geq 4/\sqrt{5} = 1.7889$ along the axes u and v, and $r_c/r_s \geq 2\sqrt{3}/\sqrt{5} = 1.5492$ along the axis w. Since we need to communicate along all three axes in order to maintain connectivity, the minimum communication range must be the maximum of the minimums along all three axes. The results are summarized in Table II.

6. Full Coverage and Connectivity for All Values of r_c/r_s

From the results of previous section, it is clear that TO model provides full connectivity only when $r_c/r_s \geq 4/\sqrt{5}$. None of the four models has full connectivity with all first-tier geographically neighboring nodes for all values of r_c/r_s. So to ensure full coverage and full connectivity for all values of r_c/r_s, we modified the models as follows:

Modified TO placement strategy. In original TO model, maximum distance between any two neighboring nodes is $4R/\sqrt{5}$, where R is the radius of a cell. So to achieve connectivity along all three axes for all values of r_c/r_s, in *modified* TO, we set $R = \min(r_c\sqrt{5}/4, r_s)$.

Modified HP placement strategy. In original HP model, maximum distance between any two neighbors along the plane that has hexagonal tessellation is $a\sqrt{3}$, where a is the length of each side of a hexagonal face of a hexagonal prism. Now, if $r_c/r_s \geq \sqrt{2}$, in order to maintain connectivity, we must have $a = r_s\sqrt{2}/\sqrt{3}$. So in *modified* HP we set $a = \min(r_c/\sqrt{3}, r_s\sqrt{2}/\sqrt{3})$ for the general case. In original HP, when $r_c/r_s \geq \sqrt{2}$, the distance between any two neighbors along the height axis is $h = 2\sqrt{r_s^2 - a^2}$. So in order to ensure connectivity for all values of r_c/r_s, we must have $h = \min(r_c, 2\sqrt{r_s^2 - a^2})$ in *modified* HP. We can achieve *modified* HP placement in the following way:

Take any arbitrary point (x, y, z) as the center of the network and deploy one node in co-ordinate

$$\Big(x + u \times a\sqrt{3}\sin 60^\circ, y + u \times a\sqrt{3}\cos 60^\circ + v \times a\sqrt{3}, z + w \times h\Big)$$

where $u \in Z$, $v \in Z$, $w \in Z$, and Z is set of all integers.

DOI: 10.1002/wcm

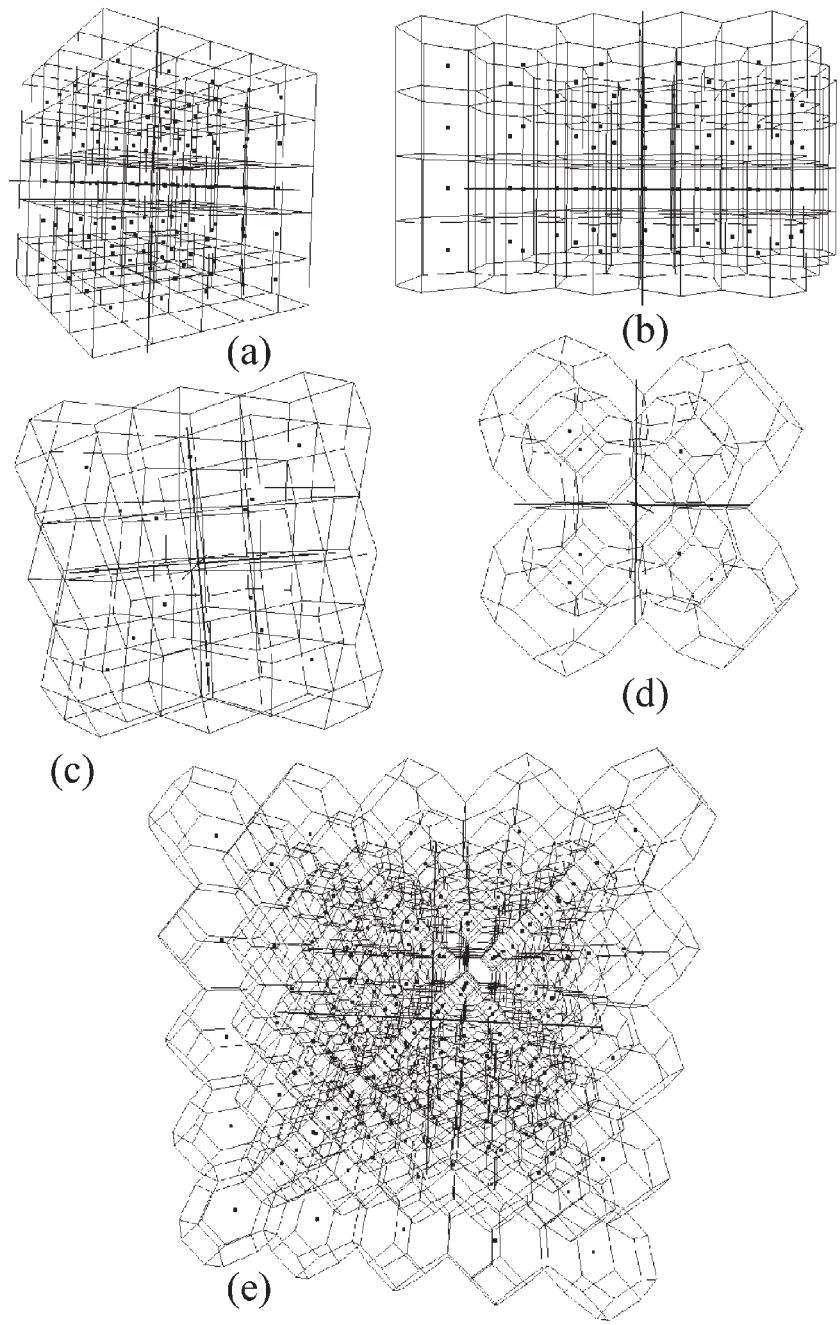

Fig. 5. Node placement under different models. (a) CB, (b) HP, (c) RD, (d) and (e) TO. Each black dot inside each cell represents the location of a node.

Modified RD placement strategy. In original RD model, distance between any two first-tier neighbors is always $R\sqrt{2}$, where R is the radius of a cell. So connectivity with all neighbors can be achieved for all values of r_c/r_s, if we set $R = \min(r_c/\sqrt{2}, r_s)$ in *modified* RD.

Modified CB placement strategy. In original CB model, distance between any two first-tier neighbors is always $2R/\sqrt{3}$, where R is the radius of a cell. So connectivity with all neighbors can be achieved for all values of r_c/r_s, if we set $R = \min(r_c\sqrt{3}/2, r_s)$ in *modified* CB.

DOI: 10.1002/wcm

Table II. Minimum communication range r_c for different models.

Model	Minimum r_c			Max of Min r_c
	u-axis	*v*-axis	*w*-axis	
CB	$1.1547r_s$	$1.1547r_s$	$1.1547r_s$	$1.1547r_s$
HP	$1.4142r_s$	$1.4142r_s$	$1.1547r_s$	$1.4142R$
RD	$1.4142r_s$	$1.4142r_s$	$1.4142r_s$	$1.4142r_s$
TO	$1.7889r_s$	$1.7889r_s$	$1.5492r_s$	$1.7889r_s$

Volume and placement strategy for *modified* CB, *modified* RD, and *modified* TO are same as those of CB, RD, TO, respectively, with the values of R being set according to above discussion.

6.1. Comparison and Results

Since all values are exact, we can just plug in the values of r_c/r_s in the equations and immediately get a graph that nicely shows the performance of each placement strategy for various values of r_c/r_s (see Figure 6). In all cases, the volume of a cell (in terms of r_s^3) is a monotonically non-decreasing function of r_c/r_s. In particular, for *modified* TO, the volume of a cell is a monotonically increasing function of r_c/r_s, for all $r_c/r_s < 4/\sqrt{5} = 1.7889$. For $r_c/r_s \geq 4/\sqrt{5}$, it is constant and has the value $32r_s^3/5\sqrt{5} = 2.862r_s^3$. For both *modified* HP and *modified* RD, volume of a cell is a monotonically increasing function of r_c/r_s, for all $r_c/r_s < \sqrt{2} = 1.4142$. For $r_c/r_s \geq \sqrt{2}$, it is constant and has the value $2r_s^3$. However, as we see in Figure 6, *modified* HP has higher volume than

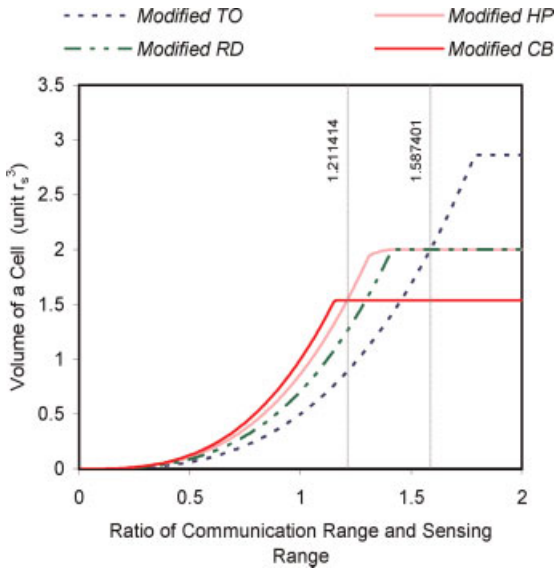

Fig. 6. Performance of various placement strategies.

modified TO for $r_c/r_s < \sqrt{2}$, because unlike *modified* RD, the distance with all neighbors are not uniform in *modified* HP. Finally, for *modified* CB, volume of a cell is a monotonically increasing function of r_c/r_s, for all $r_c/r_s < 2/\sqrt{3} = 1.1547$. For $r_c/r_s < 1.1547$, it is constant and has the value $8r_s^3/3\sqrt{3} = 1.5396r_s^3$. Since the number of nodes required by any placement strategy is inversely proportional to the volume of a cell, we can conclude the following:

- if $r_c/r_s \geq 1.587401$, then *Modified* TO is the best strategy,
- if $1.587401 > r_c/r_s \geq 1.211414$, then *Modified* HP is the best strategy, and
- if $r_c/r_s < 1.211414$, then *Modified* CB (3D grid-based placement) is the best strategy.

7. Full Coverage and 1-Connectivity for All Values of r_c/r_s

The overhead in terms of the number of nodes needed to achieve full connectivity with all geographically neighboring nodes is prohibitively high when the value of r_c/r_s is small. In such a network, full coverage can be achieved with smaller number of nodes if the requirement of full connectivity with all geographically neighboring nodes is relaxed. Relaxing full connectivity requirement means communication among distant nodes in general takes longer route and if nodes are failure prone, there is a chance that some nodes may be totally disconnected. So here we have a trade-off between faster and reliable communication and the number of nodes needed. Relaxing full connectivity with all first-tier neighboring nodes makes sense when the nodes are expensive and robust with very low probability of failure, and the value of r_c/r_s is small.

In this section, we provide a strip-based placement strategy for 3D network that provides full coverage and 1-connectivity when $r_c/r_s < 4/\sqrt{5}$ inspired by the scheme used in Reference [2] for 2D networks. This approach automatically provides full coverage and full connectivity with all neighboring nodes with minimum number of nodes when communication range is sufficiently high (i.e., $r_c/r_s \geq 4/\sqrt{5}$).

We can achieve full coverage and 1-connectivity with minimum number of nodes in the following strip-based node placement in 3D. Set distance between any two nodes in a strip as $\alpha = \min\{r_c, 4r_s/\sqrt{5}\}$ and keep distance between two parallel strips in a plane as $\beta = 2\sqrt{r_s^2 - (\alpha/4)^2}$ (see Figure 7). Set distance

DOI: 10.1002/wcm

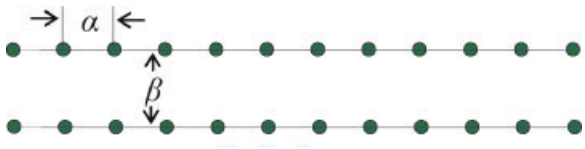

Fig. 7. Nodes in a particular plane.

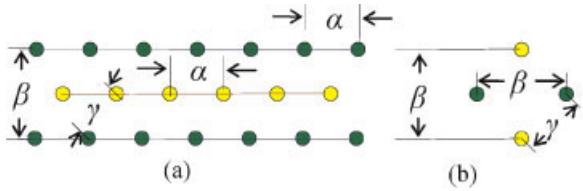

Fig. 8. (a) Horizontal and (b) vertical projection of nodes in two different planes (nodes with the same color are from the same plane).

between two planes of strips as $\beta/2 = \sqrt{r_s^2 - (\alpha/4)^2}$ and deploy strips such that a strip of one plane is placed between two strips of a neighboring plane (see Figure 8). Here distance between two neighboring nodes that reside in two different plane is $\gamma = \sqrt{\beta^2/2 + \alpha^2/4}$.

This deployment of sensors can be achieved by taking any arbitrary co-ordinate (x, y, z) as the center of the network and placing a node at each of the coordinates

$$(x + u\alpha + w\gamma\cos\theta, y + v\beta + w\gamma\cos\theta, z + w\gamma\cos\theta)$$

where $\theta = \cos^{-1}(\sqrt{1/3})$ and $u \in Z$, $v \in Z$, $w \in Z$; Z is the set of all integers.

Some additional nodes have to be deployed to achieve connectivity among different strips as described at the end of this section.

If $r_c/r_s \geq 4/\sqrt{5}$, we have $\alpha = \beta = 4r_s/\sqrt{5}$ and $\gamma = 2\sqrt{3}r_s/\sqrt{5}$, which is identical to that of optimal TO model. If $r_c/r_s < 4/\sqrt{5}$, we have $\alpha = r_c$, $\beta = 2\sqrt{r_s^2 - (r_c/4)^2}$, and $\gamma = \sqrt{2r_s^2 + r_c^2/8}$. Then we have to place a node at each coordinate

$$\begin{pmatrix} x + ur_c + w\sqrt{2r_s^2/\sqrt{3} + r_c^2/8\sqrt{3}}, \\ y + 2v\sqrt{r_s^2 - (r_c/4)^2} + w\sqrt{2r_s^2/\sqrt{3} + r_c^2/8\sqrt{3}}, \\ z + w\sqrt{2r_s^2/\sqrt{3} + r_c^2/8\sqrt{3}} \end{pmatrix}$$

where $u \in Z$, $v \in Z$, $w \in Z$, and Z is the set of all integers.

7.1. Analysis

Here, we describe how we come up with the values of the parameters: α, β, γ. We can ensure 1-connectivity by ensuring each node in a strip is connected to both of its neighbors in the strip. Since maximum distance between any two neighbors in original TO model is $4r_s/\sqrt{5}$, we can ensure connectivity as well as optimality (when $r_c \geq 4r_s/\sqrt{5}$) by setting $\alpha = \min\{r_c, 4r_s/\sqrt{5}\}$. Once we ensure connectivity along the strip, we do not need to worry about connectivity when we determine the value of β. We rather want β to be as large as possible as long as we have full coverage. In 2D case, the calculation of the value of β is simpler as all points between two strips must be within the sensing range of at least one node residing on the two strips. However, in a 3D network this is not true anymore. In 3D, nodes residing on other planes (both above and below) provide coverage for some area between the two strips. This is illustrated in Figure 9. The area inside the dotted inner circle with diameter d_2 is covered by the nodes placed in one level above and one level below. From Figure 9, we have $\alpha = d_1 + d_2 + d_3$, where $d_1 = d_3 = \sqrt{r_s^2 - \beta^2/4}$.

Next, we use a symmetry argument to find the value of d_2. If we rotate the network by 90°, then the network looks identical to the network before rotation; however, the nodes that were in one level above and one level below would now be in the same plane and so the distance between them must be β (the two nodes are in the same plane but in different strips). Now let us go back to our network before rotation. Since the distance between the nodes in one level above and one level below is β, then again by symmetry, the height of the node in the above level is $\beta/2$.

Then we have $d_2 = 2\sqrt{r_s^2 - \beta^2/4}$ (see Figure 9(b)). Substituting the value of d_2, we have $\alpha = d_1 + d_2 + d_3 = 4\sqrt{r_s^2 - \beta^2/4}$, which implies $\beta = 2\sqrt{r_s^2 - (\alpha/4)^2}$.

We can calculate the distance between two neighboring nodes that reside in two different planes (e.g., distance between any one of the four nodes in Figure 9(a) and the node in one level above that covers the inner circle) as follows: distance from any of the four nodes to the center of the inner circle is $\sqrt{\alpha^2 + \beta^2}/2$. Then, we have $\gamma = \sqrt{\beta^2/2 + \alpha^2/4}$ (see Figure 9(c)).

7.2. Auxiliary Nodes

Unless $\beta \leq r_c$ or, $\gamma \leq r_c$, this strip based approach only ensures connectivity among nodes in the same strip. In order to ensure connectivity between strips, we need to place additional nodes between strips. We can achieve 1-connectivity by placing auxiliary nodes

DOI: 10.1002/wcm

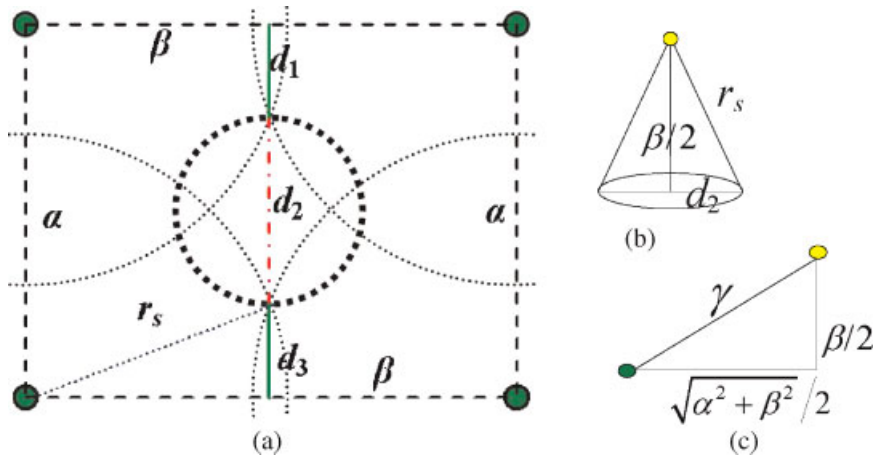

Fig. 9. (a) Cross-section along a plane. Inner dotted circle is the area covered by a node placed in the planes one level above and below. (b) Calculation of d_2. (c) Calculation of γ.

such that any two neighboring nodes in two strips are connected. However, 2-connectivity can only be achieved by placing auxiliary nodes at the two endpoints of the strips along the boundary of the network. Unless $\beta \leq r_c$ or, $\gamma \leq r_c$, there is no way to achieve 3- or higher connectivity without deploying a large number of auxiliary nodes.

8. Discussions

In this section, we provide some high-level discussion on how our placement strategies can be adjusted for real-world situations where some of our assumptions may be violated.

Our assumptions of sphere-based sensing, sphere-based communication (disk based in 2D), and homogenous sensing and communication range of each sensor are standard assumptions in most network modeling works. In the case of irregular sensing and communication range of nodes, one simple solution is to conservatively estimate the sensing range and communication range so that above assumptions remain true. For example, suppose that the sensing (communication) range is irregular but the minimum sensing (communication) range of each node is known to be $r_s^{min}(r_c^{min})$, then the network designer can set $r_s(r_c)$ to $r_s^{min}(r_c^{min})$ and use the technique provided in this paper. The loss of efficiency in this conservative estimation depends on the degree of irregularity in the sensing and communication range. A comprehensive analysis is an interesting future work.

Our assumption of no boundary effect cannot be valid in practice as all real networks will be finite in size. However, if the height, width and length of the network is significantly larger than the sensing range of each node, then 3D space of any shape can be covered with any virtual cell shape with small overhead near the boundary. The smaller the sensing range, the smaller the boundary effect and the boundary effect vanishes when the sensing range becomes infinitesimally small. Figure 10 shows how a 3D cube-shaped space is covered by a network consisting of $20 \times 20 \times 20$ nodes placed under TO model. This illustration is made in C using OpenGL following TO *model* node deployment strategy of this paper.

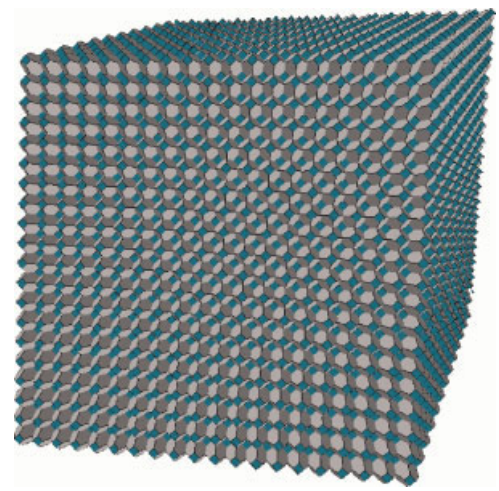

Fig. 10. Coverage of a cube shape 3D space in TO model with $20 \times 20 \times 20$ nodes.

DOI: 10.1002/wcm

Finally, the adjustable node position assumption is unlikely to be valid in a real underwater sensor network. Precise positioning in underwater is extremely difficult as GPS does not work underwater. However, our work does not require absolute positioning mechanism, rather any relative positioning mechanism where a node knows its position relative to the seed node is sufficient. Again, in many sensor network applications (e.g., detection, monitoring) it is important to know from where any piece of information originates. Any underwater sensor network that is deployed for such application must have some positioning component and our node placement strategy can get the position information from such component without adding any extra overhead. Localization and positioning in underwater is an active area of research and we may have some good positioning mechanism for underwater sensor network in near future. However, any such positioning mechanism is likely to have some error in determining the position of a node. An underwater sensor network designer can accommodate any potential error by setting the sensing range and communication range of each sensor to a fraction of the actual sensing and communication range. Clearly, the value of this fraction depends on the magnitude of the positioning error. Thus by setting the sensing and communication range to a lower than actual value, we can accommodate small violation of sphere-based sensing, sphere-based communication, homogeneous sensing and communication, and adjustable node position assumptions.

9. Conclusions

In this paper, we provide a solution for coverage and connectivity problem of 3D underwater sensor networks for any ratio of communication range, r_c and sensing range, r_s. In particular, we establish that if $r_c/r_s \geq 1.587401$, then *modified* TO placement; if $1.587401 > r_c/r_s \geq 1.211414$, then *modified* HP placement, and if $r_c/r_s < 1.211414$, then *modified* CB placement model achieve full coverage and full connectivity with all geographically neighboring nodes by deploying minimum number of sensor nodes among the four models considered in this paper. This result is most significant when $r_c/r_s < 1.211414$. Since *modified* CB model is the simplest and has the least boundary effect, in practice, network designers might be tempted to use grid like placement of sensor nodes in 3D. The good news for them is that this simple placement strategy requires minimum number of nodes if $r_c/r_s < 1.211414$. We also provide a solution for the case when the value of r_c/r_s is very small and instead of maintaining full connectivity with all geographically neighboring nodes, full coverage with 1-connectivity with fewer number of nodes are more cost-effective and desirable. While we conjecture that these strategies require minimum number of nodes to achieve full coverage and the respective communication redundancy requirements, a rigorous proof of this conjecture is yet to be found.

References

1. Akyildiz IF, Pompili D, Melodia T. Underwater acoustic sensor networks: research challenges. *Ad Hoc Networks Journal* 2005; **3**(3): 257–279.
2. Bai X, Kumar S, Yun Z, Xuan D, Lai TH. Deploying wireless sensors to achieve both coverage and connectivity. In *Proceedings of ACM MobiHoc*, 2006.
3. Meguerdichian S, Koushanfar F, Potkonjak M, Srivastava MB. Coverage problems in wireless ad-hoc sensor networks. *INFOCOM'01*, 2001, pp. 1380–1387.
4. Xing G, Wang X, Zhang Y, Lu C, Pless R, Gill CD. Integrated coverage and connectivity configuration for energy conservation in sensor networks. *TOSN*, Vol. 1 (1), 2005.
5. Zhang H, Hou JC. Maintaining sensing coverage and connectivity in large sensor networks. *Wireless Ad Hoc and Sensor Networks: An International Journal* 2005; **1**(1–2): 89–124.
6. Varshney P. *Distributed Detection and Data Fusion*. Springer-Verlag: New York, NY, 1996.
7. Li D, Wong K, Hu YH, Sayeed A. Detection, classification and tracking of targets in distributed sensor networks. *IEEE Signal Processing Magazine* 2002; **19**(2): 17–29.
8. Couqueur T, Phipatanasuphorn V, Ramanathan P, Saluja KK. Sensor deployment strategy for target detection. In *Proceeding of the First ACM International Workshop on Wireless Sensor Networks and Applications*, September 2002; pp. 169–177.
9. Chakrabarty K, Iyengar SS, Qi H, Cho E. Grid coverage for surveillance and target location in distributed sensor networks. *IEEE Transactions on Computers* 2002; **51**(12): 1448–1453.
10. Kershner R. The number of circles covering a set. *American Journal of Mathematics* 1939; **61**: 665–671.
11. Carle J, Myoupo JF, Semé D. A basis for 3-D cellular networks. In *Proceedings of the 15th International Conference on Information Networking*, 2001.
12. Decayeux C, Semé D. A new model for 3-D cellular mobile networks, *ISPDC/HeteroPar* 2004.
13. Barnes ES, Sloane NJA. The optimal lattice quantizer in three dimensions. *SIAM Journal of Algebraic Discrete Methods* 1983; **4**: 30–41.
14. Alam SMN, Haas Z. Coverage and connectivity in three-dimensional networks. In *Proceedings of ACM MobiCom*, 2006.
15. Aristotle. *On the Heaven*, Vol. 3, Chapter 8, 350BC.
16. Hilbert D, Cohn-Vossen S. *Geometry and the Imagination.* Chelsea: New York, 1999.
17. Křížek M. Superconvergence phenomena on three-dimensional meshes. *International Journal of Numerical Analysis and Modeling* 2005; **2**(1): 43–56.
18. Steinhaus H. *Mathematical Snapshots* (3rd edn). Oxford University Press: Oxford, UK, 1969.
19. Gardner M. *The Sixth Book of Mathematical Games from Scientific American.* University of Chicago Press: Chicago, IL, 1984.
20. Wells D. *The Penguin Dictionary of Curious and Interesting Geometry.* Penguin: London, 1991.
21. Johnson NW. *Uniform Polytopes.* Cambridge University Press: Cambridge, England, 2000.

DOI: 10.1002/wcm

22. Thomson W (Lord Kelvin). On the division of space with minimum partition area. *Philosophical Magazine* 1887; **24**: 503–514. Web: http://zapatopi.net/kelvin/papers/on_the_division_of_space.html
23. Weyl H. *Symmetry.* Princeton University Press: Princeton, NJ, 1952.
24. Weaire D. *The Kelvin Problem: Foam Structures of Minimal Surface Area.* Taylor and Francis: London, 1996.
25. Weaire D, Phelan R. A counter-example to Kelvin's conjecture on minimal surfaces. *Philosophical Magazine Letters* 1994; **69**: 107–110.
26. Hales TC. A proof of the Kepler conjecture. *Annals of Mathematics* 2005; **162**: 1065–1185.
27. Lynch N. *Distributed Algorithms*. Morgan Kaufmann Publishers: Wonderland, 1996.

Authors' Biographies

S. M. Nazrul Alam is a Ph.D. Candidate in the Department of Computer Science at Cornell University. He obtained his M.S. in Computer Science from the University of Toronto in 2004 and B.S. in Computer Science and Engineering from Bangladesh University of Engineering and Technology (BUET) in 2002. He also received a Master degree from Cornell University. He was awarded University Gold Medal and Sharfuddin Gold Medal by BUET for obtaining the highest CGPA in the whole university and in CSE department, respectively. His research interest is in the area of 3-D networks and underwater sensor networks. He is also interested in quantitative finance and has finished his Ph.D. minor in Finance.

Zygmunt J. Haas received his B.Sc. in EE in 1979 and M.Sc. in EE in 1985. In 1988, after earning his Ph.D. from Stanford University, he joined the AT&T Bell Laboratories, Network Research Department. There he pursued research on wireless communications, mobility management, fast protocols, optical networks, and optical switching. From September 1994 till July 1995, Dr. Haas worked for the AT&T Wireless Center of Excellence, where he investigated various aspects of wireless and mobile network technologies. In August 1995, he joined the faculty of the School of Electrical and Computer Engineering at Cornell University, where he is now a Professor. He is an author of numerous technical conference and journal papers and holds eighteen patents in the areas of highspeed networking, wireless networks, and optical switching. He has organized several workshops, delivered numerous tutorials at major IEEE and ACM conferences, and serves as editor of several journals and magazines, including the *IEEE Transactions on Networking*, the *IEEE Transactions on Wireless Communications*, the *IEEE Communications Magazine*, and the *ACM/Kluwer Wireless Networks Journal*. He has been a guest editor of IEEE JSAC issues on 'Gigabit Networks,' 'Mobile Computing Networks,' and 'Ad-Hoc Networks.' Dr. Haas served as a Chair of the IEEE Technical Committee on Personal Communications and is currently serving as the Chair of the Steering Committee of the IEEE Pervasive Computing magazine. Dr. Haas is an IEEE Fellow. His interests include: mobile and wireless communication and networks, performance evaluation of large and complex systems, and biologically inspired networks. His URL is: http://wnl.ece.cornell.edu.

DOI: 10.1002/wcm